

# Solid Solution Precursors to Gadolinia-Doped Ceria Prepared via a Low-Temperature Solution Route

Yong Bok Go and Allan J. Jacobson\*

Department of Chemistry, University of Houston, Houston, Texas 77204-5003

Received May 14, 2007. Revised Manuscript Received July 11, 2007

The conditions for the high-yield preparation of two crystalline solid solution precursors to high-purity gadolinia-doped ceria (GDC) powder have been systematically investigated. Cerium–gadolinium solid solution formate and carbonate precursors were obtained directly from solution in crystalline form with small particle size, and their decomposition behavior was determined. The morphology of the precursor crystals and the GDC powders obtained by their decomposition were found to be influenced by the reactants, reaction temperature, and the reaction method. The GDC powders were easily densified, and the measured ionic conductivities are comparable to the best literature data.

## Introduction

Ceria-based electrolytes are of current interest for application in intermediate temperature–solid oxide fuel cells (IT-SOFCs) because of their high ionic conductivity. Gadolinia-doped ceria (GDC,  $\text{Ce}_{0.9}\text{Gd}_{0.1}\text{O}_{2-\delta}$ ), for example, has significantly higher ionic conductivity than that of yttria-stabilized zirconia. At high temperatures ( $>600^\circ\text{C}$ ), GDC has significant electronic conductivity in reducing conditions, but the electronic contribution to the total conductivity decreases with decreasing temperature and, consequently, GDC is an excellent candidate for use in IT-SOFCs operating in the range of  $500 - 600^\circ\text{C}$ .

Conventionally, GDC is made by a ceramic technique in which  $\text{CeO}_2$  and  $\text{Gd}_2\text{O}_3$  powders are mixed in a ball-mill, pressed, and sintered for a few hours at ca.  $1700 - 1800^\circ\text{C}$ . The process typically gives ceramics with densities close to 90% of the theoretical value and grain sizes larger than  $10\ \mu\text{m}$ .<sup>1</sup> For application as an electrolyte in SOFCs, higher densities and lower processing temperatures are preferred. In an attempt to lower the sintering temperature and to obtain higher density ceramics, solution methods via precursor routes or sol–gel processes<sup>2</sup> have been used to obtain smaller GDC particles. Several solution-based approaches have been reported including the use of the Pechini technique,<sup>3</sup> precipitation methods,<sup>4</sup> and hydrothermal synthesis.<sup>5</sup> Solution methods have the advantage that the stoichiometry and purity can be controlled precisely, leading to a precursor and ultimately an end-product of high purity, high yield, and a uniform regular morphology with a narrow particle size

distribution. Most solution methods involve the synthesis of a precursor that can be thermally decomposed to the product ceramic powder at moderate temperatures in the range of  $300 - 400^\circ\text{C}$ .

A good precursor should be easy and inexpensive to make with a defined stoichiometry, homogeneous in composition, pure, and decompose at low temperature to a powder that can be easily densified. The particle size of the precursor should be small because the morphology of the final ceramic powder usually depends on that of the precursor. For example, it has been reported that the size and shape of  $\text{Ce}(\text{OH})(\text{CO}_3)$  precursor crystals do not change after heat treatment at  $500^\circ\text{C}$  for 1 h to give  $\text{CeO}_2$ .<sup>6</sup>

GDC has been made previously by the pyrolysis of cerium and gadolinium oxalates at  $1000^\circ\text{C}$  for 1 h<sup>7</sup> and from crystalline formate precursors. The latter were made by the reaction of an ethylene glycol solution of the nitrates with concentrated nitric acid by heating at  $80^\circ\text{C}$  for about 200 h. Further heating this solution for 437 h resulted in the formation of GDC, showing the possibility of the direct formation of GDC powder via a polymerized precursor solution.<sup>8</sup> Fujihara et al. reported the synthesis of cerium carbonate including samarium-doped cerium carbonate.<sup>9</sup> In their report,  $\text{Ce}(\text{NO}_3)_3 \cdot 6\text{H}_2\text{O}$  and urea were dissolved in deionized water and the solution was heated at  $80^\circ\text{C}$  for 24 h.  $\text{Ce}_2\text{O}(\text{CO}_3)_2 \cdot \text{H}_2\text{O}$  was precipitated as rod-shaped particles (approximately  $5 \times 2\ \mu\text{m}$ ) as a result of fast crystal growth in the solution. When  $\text{CeCl}_3 \cdot 6\text{H}_2\text{O}$  was used instead of nitrate, triangular prism-shaped particles (approximately  $20 - 30\ \mu\text{m}$  in height and  $5 - 10\ \mu\text{m}$  in thickness) were precipitated.

In this work, we have systematically investigated two solid solution precursor routes to GDC powders with high yield,

\* To whom correspondence should be addressed. E-mail: ajacob@uh.edu. Telephone: (713) 743-2785. Fax: (713) 743-2787.

- (1) (a) Kudo, T.; Obayashi, H. *J. Electrochem. Soc.* **1976**, *123* (3), 415–419. (b) Kudo, T.; Obayashi, H. *J. Electrochem. Soc.* **1975**, *122* (1), 142–147.
- (2) Huang, K.; Feng, M.; Goodenough, J. B. *J. Am. Ceram. Soc.* **1998**, *81*, 357.
- (3) Pechini, M. P. U.S. Patent 3,330,697, 1967.
- (4) (a) Hsu, W. P.; Ronnquist, L.; Matijevic, E. *Langmuir* **1988**, *4*, 31–37. (b) Matijevic, E. *Chem. Mater.* **1993**, *5*, 412. (c) Matijevic, E.; Hsu, W. P. *J. Colloid Interface Sci.* **1987**, *118*, 506.
- (5) Dawson, W. J. *Ceram. Bull.* **1988**, *67*, 1673.

(6) Wang, H.-C.; Lu, C.-H. *Mater. Res. Bull.* **2002**, *37*, 783.

(7) (a) Riess, I.; Braunshtein, D.; Tannhauser, D. S. *J. Am. Ceram. Soc.* **1981**, *64*, 479. (b) Overs, A.; Riess, I. *J. Am. Ceram. Soc.* **1982**, *65*, 606.

(8) Wang, S.; Maeda, K. *J. Am. Ceram. Soc.* **2002**, *85* (7), 1750.

(9) Oikawa, M.; Fujihara, S. *J. Sol. State Chem.* **2005**, *178*, 2036.

high purity, and small particle size. The syntheses of both formate and carbonate precursors from solution in crystalline form and their decomposition behavior have been examined. The morphology of the precursor crystals and the GDC powders obtained by their decomposition were found to be influenced by the reactants and reaction temperature. The GDC powders were densified, and the ionic conductivity was measured and compared with literature data.

### Experimental Section

**Materials.** All reactants were reagent-grade and were used as purchased without further purification. Cerium(III) nitrate hexahydrate ( $\text{Ce}(\text{NO}_3)_3 \cdot 6\text{H}_2\text{O}$ ; 99%, Aldrich), cerium(III) chloride hexantrate ( $\text{CeCl}_3 \cdot 6\text{H}_2\text{O}$ ; 99.9%, Aldrich), gadolinium(III) nitrate hexahydrate ( $\text{Gd}(\text{NO}_3)_3 \cdot 6\text{H}_2\text{O}$ ; 99.9%, Aldrich), gadolinium acetate hydrate ( $\text{Gd}(\text{OAc})_3 \cdot x\text{H}_2\text{O}$ ; 99.9%, Aldrich), formic acid, and urea (99+ %, Aldrich) were used as starting materials.

**Typical Syntheses.** *The Formate Precursor*  $\text{Ce}_{0.9}\text{Gd}_{0.1}(\text{HCOO})_3$ .  $\text{Ce}(\text{NO}_3)_3 \cdot 6\text{H}_2\text{O}$  (5.520 g, 12.71 mmol),  $\text{Gd}(\text{NO}_3)_3 \cdot 6\text{H}_2\text{O}$  (0.636 g, 1.41 mmol), and  $\text{HCOOH}$  (1.952 g, 42.38 mmol) were dissolved in a mixture of DMF/EtOH/ $\text{H}_2\text{O}$  (20/15/25 mL), and this clear solution was refluxed at 105 °C for 12 h with vigorous stirring to give short rod-shaped white crystals of the formate. The white crystals were filtered and washed with water and ethanol. Yield: 97% based on Ce.

*The Carbonate Precursor*  $\text{Ce}_{0.9}\text{Gd}_{0.1}(\text{OH})(\text{CO}_3)$ .  $\text{Ce}(\text{NO}_3)_3 \cdot 6\text{H}_2\text{O}$  (5.520 g, 12.71 mmol),  $\text{Gd}(\text{NO}_3)_3 \cdot 6\text{H}_2\text{O}$  (0.636 g, 1.41 mmol), and urea (2.12 g, 35.30 mmol) were dissolved in deionized water, and the concentration of metal ions and urea was adjusted to 0.2 and 0.5 M, respectively. The reaction vessel was placed in a silicone oil bath, and the clear solution was refluxed at 105 °C for 12 h with vigorous stirring. The white crystalline powder was filtered and washed with water and ethanol. Yield: 99% based on Ce. Parallelogram-shaped colorless crystals of  $\text{Ce}_{1.8}\text{Gd}_{0.2}(\text{CO}_3)_3 \cdot 8\text{H}_2\text{O}$  (**3**) were obtained as a major phase when the same reaction mixture was heated in a sealed tube at 100 °C for 1 h then isolated at room temperature for 3 days.

**Preparation of GDC from Precursors.** Both formate and carbonate were heat-treated in air at 350 °C for 10 h to give yellow GDC powder.

**Characterization.** The precursor and GDC particle morphologies were observed by scanning electron microscopy (SEM-JEOL 8300). The thermal decomposition behaviors of  $\text{Ce}_{0.9}\text{Gd}_{0.1}(\text{HCOO})_3$  and  $\text{Ce}_{0.9}\text{Gd}_{0.1}(\text{CO}_3)(\text{OH})$  were determined by thermogravimetric analysis (TGA) at a rate of 3 °C/min in air using a V5.1A DuPont 2100 instrument. The X-ray powder diffraction patterns of the precursors and the GDC obtained from them were collected on a Scintag XDS 2000 diffractometer with Cu K $\alpha$  radiation. Nitrogen adsorption isotherms were measured using a Coulter OMISORP 100 automated gas sorption analyzer.

**Impedance Measurements.** The GDC powders obtained by heat treatment of the precursors were cold isostatically pressed into pellets at 40 000 psi and sintered in air at 1450 °C for 10 h. The pellet densities were 92 (carbonate), 95, and 96% (formates) of the theoretical value. Pt electrodes were painted on both sides of the GDC pellet with 0.89 (carbonate), 0.75 (95% dense formate), or 0.70 (96% dense formate) cm<sup>2</sup> active area using Pt paste and were sintered at 800 °C in air for 2 h to give good adhesion at the Pt/GDC interfaces. The symmetrical Pt/GDC/Pt cell and the fine Pt gauzes (100 mesh) that were used as the current collector on both electrodes were pressed together physically with spring loading. Two-probe ac impedance measurements were made using a Solatron Instruments 1260 impedance analyzer in the frequency

Table 1. Crystallographic Data for 1–3

	1	2	3
chemical formula	$\text{C}_3\text{H}_3(\text{Ce,Gd})\text{O}_6$	$\text{CH}(\text{Ce,Gd})\text{O}_4$	$\text{C}_3\text{H}_{16}(\text{Ce,Gd})_2\text{O}_{17}$
fw	276.89	217.84	607.82
cryst syst	trigonal	orthorhombic	orthorhombic
space group	$R\bar{3}m$	$P2_12_12_1$	$Pccn$
<i>a</i> , Å	10.673(3)	8.5501(2)	8.9475(6)
<i>b</i> , Å	10.673(3)	7.3054(2)	9.5099(7)
<i>c</i> , Å	4.099(2)	5.0045(1)	16.9616(12)
$\alpha$ , deg	90	90	90
$\beta$ , deg	90	90	90
$\gamma$ , deg	120	90	90
<i>V</i> , Å <sup>3</sup>	404.37(20)	312.68(42)	1443.26(18)
<i>Z</i>	3	4	4
<i>T</i> , K	293(2)	298	293(2)
$\rho_{\text{c}}$ , g cm <sup>-3</sup>	3.411	4.650	2.797
$\mu(\text{Mo K}\alpha)$ , mm <sup>-1</sup>	8.791	15.05	6.606
R1, wR2 [ <i>I</i> > 2 $\sigma$ ( <i>I</i> )] <sup>a</sup>	0.0117, 0.0292	0.0643, 0.0913	0.0197, 0.0353
R1, wR2 (all data) <sup>a</sup>	0.0117, 0.0292	0.0643, 0.0913	0.0388, 0.0404

$$^a \text{R1} = \sum ||F_o| - |F_c|| / \sum |F_o|, \text{wR2} = [\sum w(F_o^2 - F_c^2)^2 / \sum w(F_o^2)^2]^{1/2}.$$

range of 0.1 to 3 MHz with ca. 30–40 mV amplitude electrical perturbation. Measurements were made in the temperature range of 318–700 °C.

**Crystallographic Studies.** Single crystals of suitable dimensions were used for the structure determinations of  $\text{Ce}_{0.9}\text{Gd}_{0.1}(\text{HCOO})_3$  (**1**) and  $\text{Ce}_{1.8}\text{Gd}_{0.2}(\text{CO}_3)_2 \cdot 8\text{H}_2\text{O}$  (**3**). All measurements were made with a Siemens SMART platform diffractometer equipped with a 1K CCD area detector. A hemisphere of data (1271 frames at 5 cm detector distance) was collected for each phase using a narrow-frame method with scan widths of 0.3° in  $\omega$  and an exposure time of 40 s/frame. The first 50 frames were remeasured at the end of data collection to monitor instrument and crystal stability, and the maximum correction applied to the intensities was less than 1%. The data were integrated using the Siemens SAINT program,<sup>10</sup> with the intensities corrected for Lorentz factor, polarization, air absorption, and absorption due to variation in the path length through the detector faceplate. The structure was solved by direct methods and refined on  $F^2$  by full-matrix least squares using SHELXTL.<sup>11</sup> All non-hydrogen atoms were refined anisotropically. Hydrogen atoms were refined isotropically with geometric constraints. Crystal data for **1** and **3** are summarized in Table 1.

For  $\text{Ce}_{0.9}\text{Gd}_{0.1}(\text{OH})(\text{CO}_3)$  (**2**), single crystals large enough for single-crystal X-ray diffraction could not be obtained, and consequently, the structure was determined from powder diffraction data. X-ray data were measured using a Scintag XDS 2000 diffractometer with Cu K $\alpha$  radiation in the range of  $10^\circ \leq 2\theta \leq 60^\circ$  in  $0.02^\circ$  steps with a count time of 20 s/step. The data were indexed with an orthorhombic unit cell using the program TREOR, and the space group was determined to be  $P2_12_12_1$  (No. 19). The structure of **2** was solved using the recently developed FOX software<sup>12</sup> that allows the definition of molecular fragments and uses global optimization algorithms to find their positions and orientations that give the best fit to the diffraction data and the most reasonable intermolecular contacts. The carbonate unit was introduced as a semirigid fragment, one cerium atom and one additional oxygen atom were randomly placed and oriented in the unit cell, and global optimization using parallel tempering was carried out with an integrated  $R_w$  factor cost function. This process produced a solution in which all cerium atoms had a complete coordination with an arrangement similar though not identical to that found in compound **2**. This solution was used as a starting model for a constrained Rietveld refinement

(10) SAINT, Program for Data Extraction and Reduction; Siemens Analytical X-ray Instruments, Inc.: Madison, WI, 1996.

(11) SHELXTL, Program for Refinement of Crystal Structures; Siemens Analytical X-ray Instruments, Inc.: Madison, WI, 1994.

(12) V. Favre-Nicolin and R. Černý, *J. Appl. Crystallogr.* **2002**, *35*, 734.

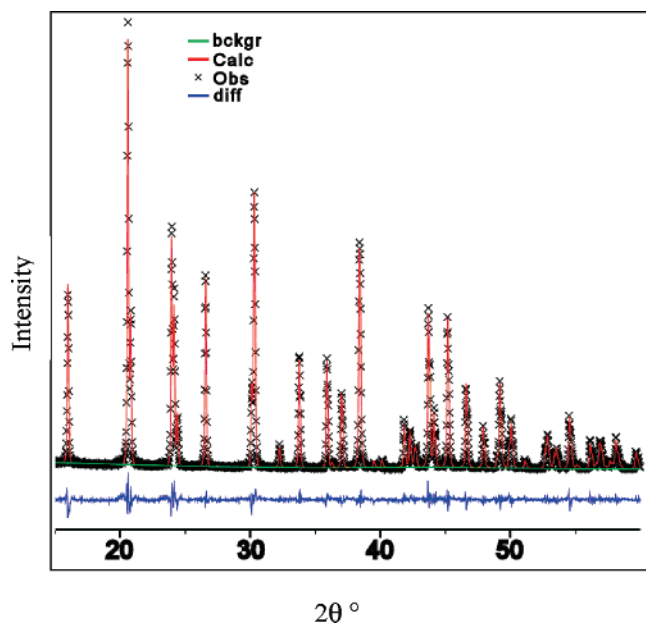


**Figure 1.** Observed, calculated, and difference powder diffraction profiles for the final Rietveld refinement of **2**.

that converged to  $\chi^2 = 2.99$ ,  $R_p = 0.0643$ ,  $R_{wp} = 0.0913$ , and  $R_{Bragg}(F^2) = 0.031$  for 128 reflections and 31 structural parameters. The profile fit is shown in Figure 1, and the results are summarized in Table 1.

## Results and Discussion

**Precursor Structures.**  $Ce_{0.9}Gd_{0.1}(HCOO)_3$  (**1**). The Ce,Gd coordination environment in **1** can be described as a tricapped trigonal prism of oxygen atoms (Figure 2). The metal center is surrounded by nine carboxylate oxygen atoms: six carboxylate oxygen atoms from formate anions bridge metal centers along the chain forming the trigonal prism, and three nonbridging oxygen atoms cap the three open faces of the prism. The closest distance between two metal centers is 4.099(2) Å along the *c* axis and 6.162(2) Å between adjacent chains. The two carboxylate oxygen atoms of the formate ligand show different coordination modes—one oxygen atom bridges two metal centers forming M—O—M pillars along the *c* axis, and the other oxygen atom connects neighboring pillars in a monodentate coordination mode. The Ce(Gd)—O bond distance with the monodentate oxygen atom is 2.494(1) Å, and the bridging oxygen atom distances range from 2.574(4) to 2.589(4) Å.

$Ce_{0.9}Gd_{0.1}(OH)(CO_3)$  (**2**). The metal center is surrounded by ten oxygen atoms: six chelating oxygen atoms forming a trigonal pyramid around a Ce(Gd) atom, two oxygen atoms from two bridging hydroxyl groups are at the opposite side of the triangle formed by three coordinated carbonate groups, and two oxygen atoms from two bridging carbonates are cis to each other (Figure 3a). The Ce(Gd)—O bond distances for the chelating carbonate oxygen atoms range from 2.536(4) to 2.770(4) Å and are 2.637(3) and 2.657(3) Å for the monodentate carbonate oxygen atoms and 2.425(1) Å for the bridging hydroxide ion. The hydroxide group bridges two metal centers forming infinite M—OH—M chains in the *ab* plane, and these chains are connected by carbonates to yield

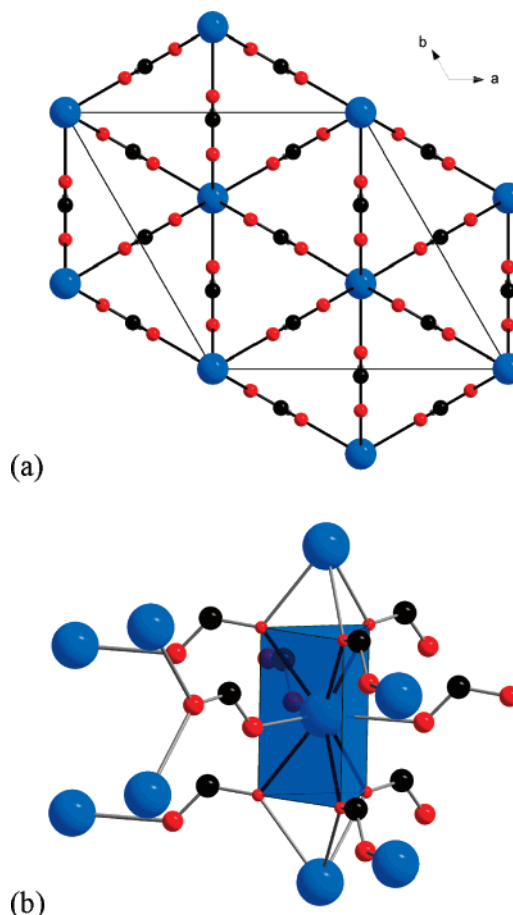


**Figure 2.** (a) Perspective view of  $(Ce_{0.9}Gd_{0.1})(HCOO)_3$  along the *c* axis and (b) of the coordination environment of a metal center showing the tricapped trigonal-prismatic geometry. Oxygen, carbon, and cerium/gadolinium atoms are shown as red, black and blue spheres, respectively.

a three-dimensional coordination polymer network with four- and eight-membered rings (Figure 3b).

$Ce_{1.8}Gd_{0.2}(CO_3)_3 \cdot 8H_2O$  (**3**). The two crystallographically distinct metal centers are surrounded by ten oxygen atoms with different coordination environments. Ce(Gd)1 is coordinated by six chelating oxygen atoms forming a triangular arrangement, two bridging oxygen atoms at the opposite side of the triangle, and two oxygen atoms from coordinated water molecules (Figure 4a). However, Ce(Gd)2 is coordinated by four oxygen atoms from two trans chelating carbonate groups, two oxygen atoms from two bridging carbonates, and four oxygen atoms from coordinated water molecules. The Ce(Gd)1—O bond distance for the bridging oxygen atom is 2.510(3) Å, for the chelating oxygen atoms ranges from 2.524(2) to 2.764(3) Å, and for the coordinated water molecules is 2.597(3) Å. The Ce(Gd)2—O bond distances for carbonate oxygen atoms range from 2.496(3) to 2.757(3) Å and for coordinated water molecules are similar to that of Ce(Gd)1—O7 ( $d_{Ce(Gd)2 \cdots O6} = 2.602(3)$  Å and  $d_{Ce(Gd)2 \cdots O8} = 2.598(3)$  Å). The extended structure layers of covalently connected metal carbonate polyhedra are connected by strong hydrogen bonds ( $d_{O5 \cdots O7} = 2.630(4)$  Å) between two coordinated water molecules and a carbonate oxygen atom from a neighboring layer (Figure 4c). The guest water molecules present in the structure have hydrogen-bonding



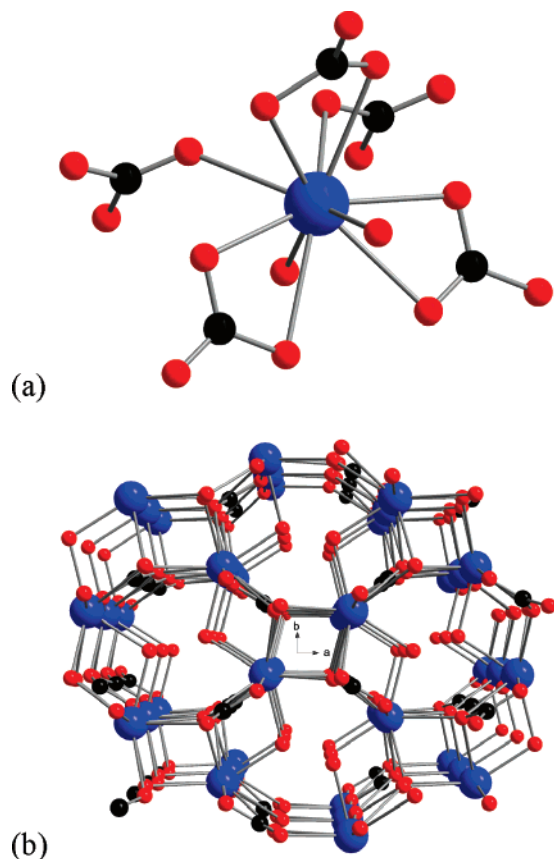


**Figure 3.** (a) Coordination environment of a metal center coordinated by 10 oxygen atoms. (b) Perspective view of  $(\text{Ce}_{0.9}\text{Gd}_{0.1})(\text{CO}_3)(\text{OH})$  along the  $c$  axis showing three-dimensional framework structure. Cerium/gadolinium, carbon, and oxygen atoms are represented by blue, black, and red spheres, respectively.

interactions with coordinated water molecules at distances ranging from 2.780(4) to 3.206(5) Å.

**Synthesis.** The precursors to  $\text{Ce}_{0.9}\text{Gd}_{0.1}\text{O}_{2-\delta}$  (GDC) were prepared via a precipitation method. Several synthesis routes were tested to obtain the maximum yield of precursors and to produce both homogeneous and small-sized crystals.

**Formate Precursor,  $\text{Ce}_{0.9}\text{Gd}_{0.1}(\text{HCOO})_3$ .** In initial experiments, GDC was made by thermal decomposition of the formate precursor, which was synthesized from the nitrates by the hydrolysis of dimethylformamide (DMF).  $\text{Ce}(\text{NO}_3)_3 \cdot 6\text{H}_2\text{O}$ ,  $\text{Gd}(\text{NO}_3)_3 \cdot 6\text{H}_2\text{O}$ , and formic acid were dissolved in a mixture of DMF/EtOH/ $\text{H}_2\text{O}$ , and this solution was refluxed at 80 °C for 12–24 h to give the needle-shaped white crystalline formate crystals with lengths of about 15  $\mu\text{m}$  (Figure 5a). Various amounts of DMF/EtOH/ $\text{H}_2\text{O}$  (5–50/0–20/0–30 mL for 12.7 mmol of  $\text{Ce}(\text{NO}_3)_3 \cdot 6\text{H}_2\text{O}$ ) were examined to find the best ratio to obtain the highest yield; each reaction was carried out at different temperatures (80, 90, or 105 °C). The maximum yield (97%, formate) was obtained when the ratio was 4:3:5 at 105 °C. At reaction temperatures of 80 and 90 °C using the same solvent ratio, the yields were 41 and 80%, respectively. Compared to the uniform needle-shaped formate crystals formed at 80 °C, the hexagonal rod-shaped crystals with lengths ranging from 1 to 10  $\mu\text{m}$  formed as the reaction temperature increased (Figure 5b).

In an attempt to produce formate crystals with an average size smaller than 10  $\mu\text{m}$  while keeping the yield high, the

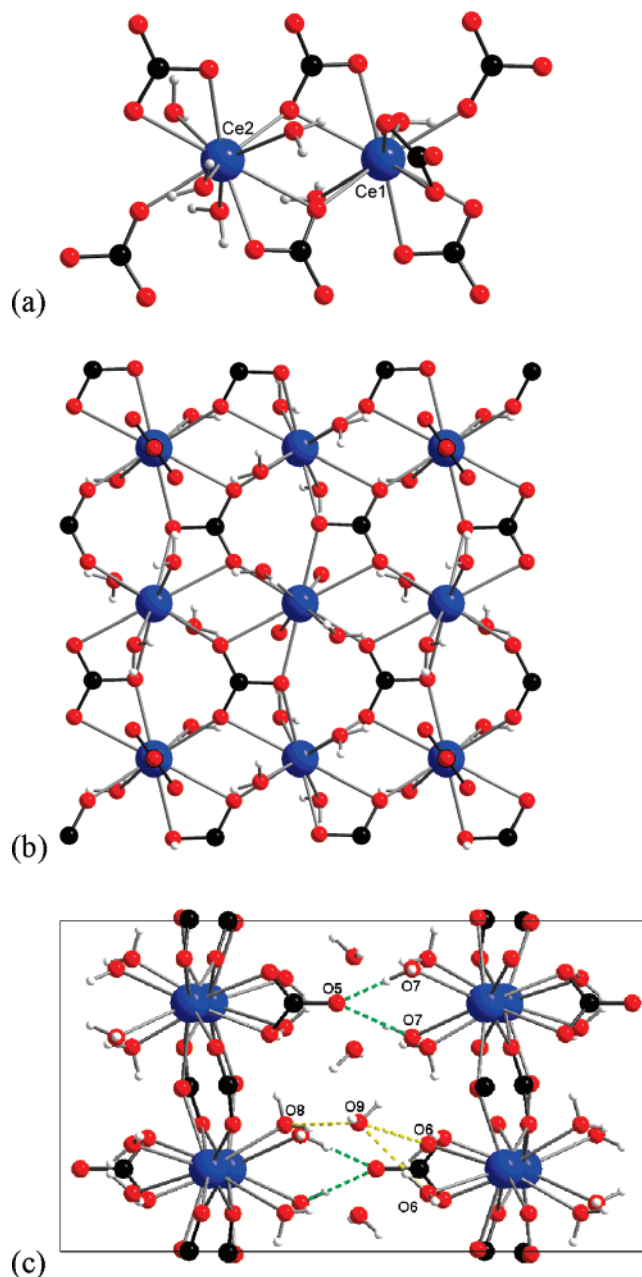


**Figure 4.** (a) Coordination environment of a metal center coordinated by 10 oxygen atoms. (b) Perspective view of  $(\text{Ce}_{1.8}\text{Gd}_{0.2})(\text{CO}_3)_3 \cdot 8\text{H}_2\text{O}$  along the  $c$  axis. (c) View of the unit cell along the  $a$  axis showing the hydrogen bonding of coordinated water molecules (green dotted lines) and guest water molecules (yellow dotted lines) between two adjacent layers. Cerium/gadolinium, carbon, oxygen, and hydrogen atoms are represented by blue, black, red, and white spheres, respectively.

influences of reactant, temperature, and reaction technique were examined in three other reactions by introducing cerium chloride and gadolinium acetate in place of one or the other nitrates. Reactions with three different combinations of reactants,  $\text{Ce}(\text{NO}_3)_3/\text{Gd}(\text{OAc})_3$ ,  $\text{CeCl}_3/\text{Gd}(\text{OAc})_3$ , and  $\text{CeCl}_3/\text{Gd}(\text{NO}_3)_3$ , were examined under the same reaction conditions used above for the  $\text{Ce}(\text{NO}_3)_3/\text{Gd}(\text{NO}_3)_3$  combination. Again, each reaction was carried out at different temperatures: 80, 90, or 105 °C. The effect of reaction temperature on the yields of formate showed the same trend as the nitrate/nitrate case, in which the yields increased with temperature. At 105 °C, the yields were almost the same as that for nitrate/nitrate, all above 95%, though the yields at lower temperature were

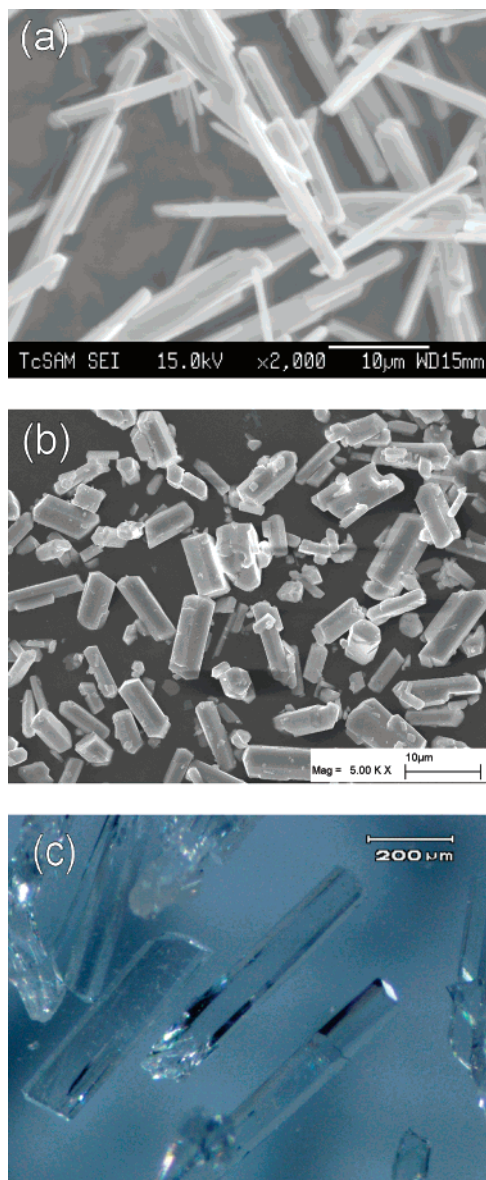


**Figure 5.** Crystals of  $(\text{Ce}_{0.9}\text{Gd}_{0.1})(\text{HCOO})_3$  prepared (a) under reflux conditions at 80 °C (SEM image), (b) at 100 °C (SEM image), or (c) in static conditions (optical image).

somewhat higher than that for nitrate/nitrate. The hexagonal rod-shaped morphology and crystal size (1–10  $\mu\text{m}$ ) of the formate crystals were also the same as those for nitrate/nitrate, regardless of the reactant combinations. When the reaction was carried out in a static reaction vessel such as a stainless-steel autoclave or sealed tube using any combination of reactants, the average crystal size was much larger, about 500  $\mu\text{m}$  at 100 °C and 50–200  $\mu\text{m}$  at 80 °C (Figure 5c).

Attempts to make the particle size of GDC small by rapidly heating the formate to 400 °C or quenching the sample after heating at 400 or 500 °C were unsuccessful because the crystal morphology was retained after such heat treatments.

**Carbonate Precursor,  $(\text{Ce}_{0.9}\text{Gd}_{0.1})_2\text{O}(\text{CO}_3)_2 \cdot \text{H}_2\text{O}$ .** To optimize the reaction conditions for high yield and small particle size of the carbonate precursor, the effects of varying the amount of urea and the temperature were examined systematically. The molar ratio of metal ions to urea was varied from 1:1 to 1:6 and the reaction mixture was heated at 80, 90, 95, 100, or 105 °C. Urea was added to an aqueous

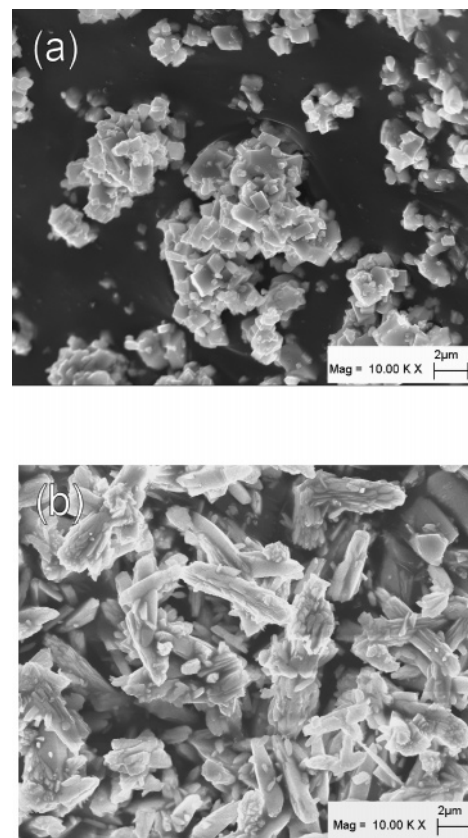


**Figure 6.** SEM images of the carbonate precursor prepared from cerium nitrate and gadolinium nitrate by (a) reflux method and (b) hydrothermal reaction.

solution of  $\text{Ce}(\text{NO}_3)_3 \cdot 6\text{H}_2\text{O}$  and  $\text{Gd}(\text{NO}_3)_3 \cdot 6\text{H}_2\text{O}$  (Ce/Gd = 9:1 in mol), and the total concentration of metal ions was adjusted to 0.2 M and fixed throughout the experiments, while the concentration of urea was varied from 0.2 to 1.2 M. The mixed solution was either heated in a stainless-steel reactor with a Teflon liner, i.e., the hydrothermal method, or refluxed in a flask with vigorous stirring, i.e., the precipitation method, at 80–105 °C for 12 h. When the ratio of metal ions to urea was 1:1 or 1:2, the yield of carbonate was about 50% regardless of the reaction temperature, suggesting that an excess of urea is needed for completion of the reaction. When the ratio was more than 1:3, the yield both increased and became temperature sensitive with a maximum yield of 99% at reaction temperature over 100 °C. In addition to such a high yield, the resulting carbonate crystals produced by the reflux method were small square blocks with dimensions of  $1 \times 1 \times 0.5 \mu\text{m}$  (Figure 6a).

When the same reaction mixture was heated under hydrothermal conditions, the yield showed the same trend but the carbonate crystals had different morphology; about 4  $\mu\text{m}$  long rough agglomerates composed of crystallites (Figure 6b).

As with the formate precursor, three other reactant metal ion pairs,  $\text{Ce}(\text{NO}_3)_3/\text{Gd}(\text{OAc})_3$ ,  $\text{CeCl}_3/\text{Gd}(\text{OAc})_3$ , and  $\text{CeCl}_3/\text{Gd}(\text{NO}_3)_3$ , were examined. The yield of carbonate in each combination increased with reaction temperature as in the case of nitrate/nitrate; the maximum yield was ca. 99% over 100 °C. Compared with the formate case, the carbonate precursor crystals show different morphologies and sizes depending on the reaction conditions and reactants. In



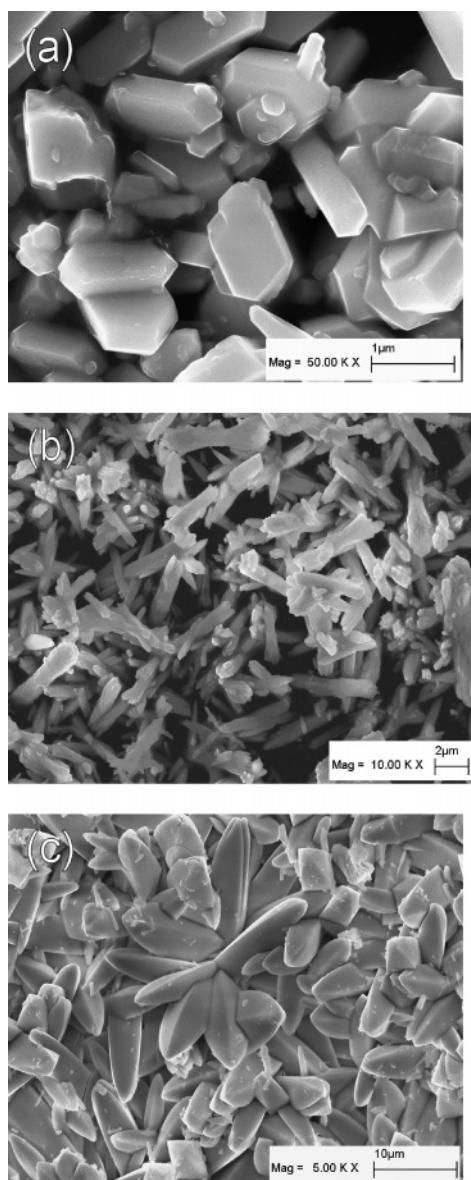


**Figure 7.** (a) SEM images of carbonate precursor prepared from chloride/acetate by reflux method, (b) hydrothermal reaction, and (c) chloride/nitrate by hydrothermal reaction.

particular, the gadolinium salt used seems to play a critical role in determining the morphology of carbonate precursor crystals. The particles were more agglomerated when gadolinium nitrate was used as a reactant. The morphology of carbonate precursor prepared from chloride/nitrate by reflux method is square plate, which is the same as that of the nitrate/nitrate case (Figure 6a), and those from nitrate/acetate or chloride/acetate are hexagonal plates (Figure 7a).

The carbonates prepared from nitrate/acetate and chloride/acetate by hydrothermal reaction are rodlike particles with lengths of  $5\ \mu\text{m}$  and widths of  $2\ \mu\text{m}$  (Figure 7b). As shown in Figure 7c, the hydrothermal reaction using chloride/nitrate leads to a peculiar morphology of the resulting carbonate precursor, which has intergrown rod-shaped crystals with average dimension of  $4 \times 4 \times 10\ \mu\text{m}$ .

It has been reported that the morphology of the undoped precursor cerium hydroxycarbonate can be changed by quenching at high temperature;<sup>13</sup> thus, when  $9\text{--}14\ \mu\text{m}$  carbonate crystals were quenched at  $500$  or  $800\ ^\circ\text{C}$ , the

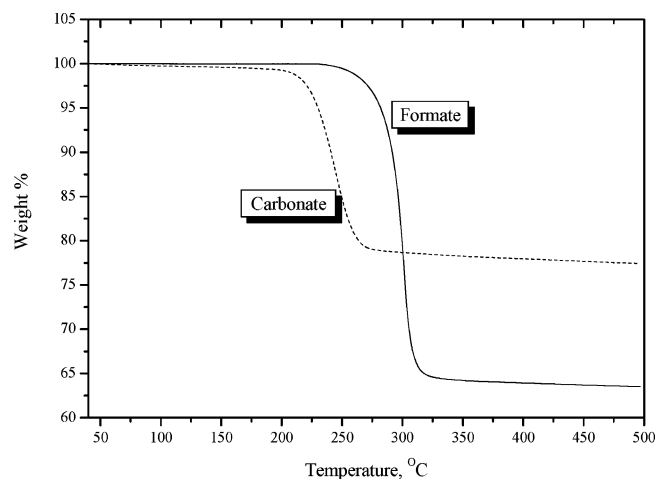


**Figure 8.** Thermal decomposition of the formate (solid line) and carbonate (dotted line) powders prepared from nitrates.

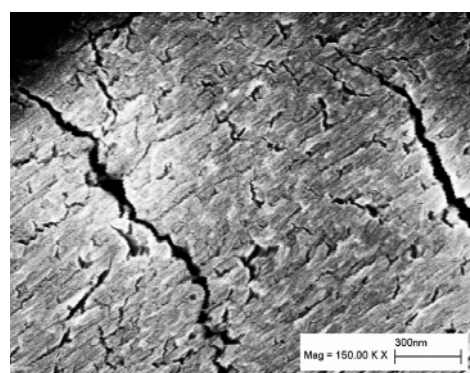


**Figure 9.** SEM image of GDC obtained by decomposition of the formate precursor at  $350\ ^\circ\text{C}$  for 12 h.

particle size was reduced to  $1.5\text{--}3$  or  $0.8\text{--}2\ \mu\text{m}$ , respectively. Because we had already achieved these small particle sizes, we did not investigate an additional quenching step.

**Thermal Decomposition.** The thermal decomposition behaviors of the two precursors were examined by TGA and are shown in Figure 8. The formate shows a one-step decomposition to GDC starting at  $270\ ^\circ\text{C}$  and complete at  $315\ ^\circ\text{C}$  (obsd. 36.87%, calcd. 37.22%), while the decomposition of the carbonate starts at  $230\ ^\circ\text{C}$  and is complete at  $280\ ^\circ\text{C}$  (obsd. 20.21%, calcd. 20.25%). The relatively low decomposition temperature of these precursors allows us to avoid high-temperature calcinations.

The decomposition of both precursors to GDC is pseudomorphic in that after the decomposition, the gross morphology of the crystals is retained. As an example, a SEM micrograph of a formate crystal after thermal decomposition is shown in Figure 9. The overall shape of the crystal is little changed, but numerous cracks and fissures have appeared as a result of the  $\text{CO}_2$  and  $\text{H}_2\text{O}$  gas evolution during the conversion. The pseudomorphic transformation presents a problem for further powder processing when the initial precursor crystals are large.

It is interesting to note that the pseudomorphic transformation is accompanied by the formation of a sample with significant surface area and relatively narrow pore-size distribution. A sample of GDC obtained from the decom-

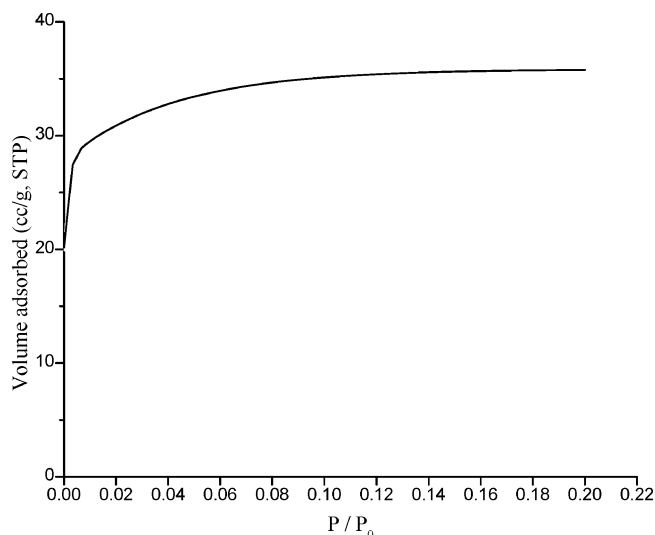


**Figure 10.**  $N_2$  gas sorption isotherm at 77 K for GDC ( $P/P_0$  is the ratio of gas pressure ( $P$ ) to saturation pressure ( $P_0$ ), with  $P_0 = 764$  Torr) obtained from the formate precursor.

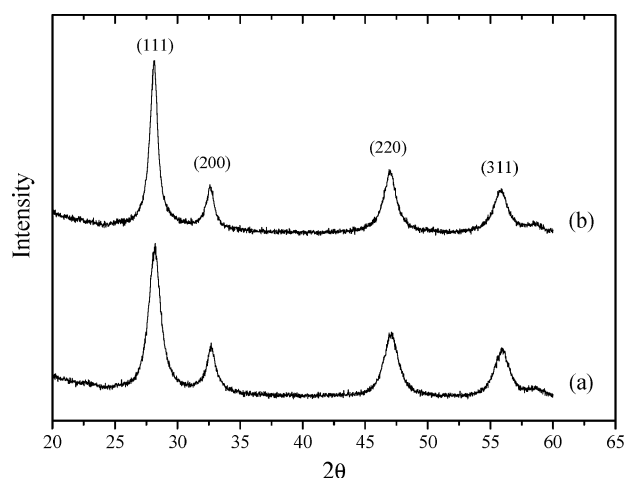


**Figure 11.** XRD patterns of the GDC powders obtained by heating (a) formate precursor and (b) carbonate precursor at 350 °C for 6 h.

position of formate was dehydrated under vacuum at 250 °C overnight, and its  $N_2$  adsorption isotherm was measured for  $P/P_0$  values up to 0.2. The total volume adsorbed was ca. 36 mL/g, and the calculated BET surface area is 123  $m^2/g$  with a pore size of  $<0.6$  nm (Figure 10). The intrinsic particle size was about 1.5 nm, which was calculated from the line broadening (Figure 11) observed in the powder X-ray data using the Scherrer formula.<sup>14</sup>

The carbonate precursor, ca. 1.0 g, was calcined for different times, 6, 4, 2, and even 1 h, at 350 °C. The crystallinity was checked by X-ray diffraction (XRD) pattern, and the intrinsic particle size (1–2.5 nm) of the resulting GDC samples were the same regardless of the calcination time, suggesting another advantage of the precursor route to GDC powder.

**Densification.** To prepare samples for electrical conductivity measurements, the conditions for the densification of GDC powder were investigated. Formate and carbonate

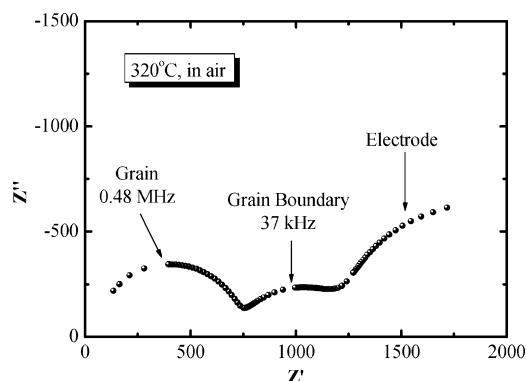


**Figure 12.** Representative impedance spectrum of gadolinia-doped ceria measured at 320 °C in air.

precursor crystals prepared from nitrate/nitrate reactant pairs in both cases with particle sizes of 1–10  $\mu m$  (Figure 5b) and 0.5–1.0  $\mu m$  (Figure 6a), respectively, were used. The precursors were heat-treated in air at 350 °C for 6–10 h to give a pale yellow GDC powder, which was cold isostatically pressed into pellets at 40 000 psi and sintered in air at 1450 °C for 10 h. The density of GDC was about 85% of the theoretical value and improved by 0.5–1% by either increasing the sintering temperature to 1500 °C or extending the sintering time to 20 h at 1450 °C. When the carbonate precursor was calcined at 850 °C for 5 h, the density of GDC was 92% of the theoretical value. Similarly, for the formate, calcining the precursor at 600 °C for 10 h resulted in a significant improvement in the density to 96%.

**Electrical Conductivity.** Measurements of ac impedance were used to determine the conductivity of the GDC samples prepared by thermal decomposition of the formate and carbonate precursors. These precursors were prepared by the reflux method using cerium nitrate and gadolinium nitrate in both cases. The detailed pellet preparation is described in the Experimental Section. As shown in Figure 12, two distinct semicircles with some distortion associated with the grain and grain-boundary response of the GDC electrolyte are seen at 318 °C at relatively high frequency ( $>2$  kHz). As the operating temperature is increased above 400 °C, the two semicircles merge together and the grain and grain-boundary processes cannot be completely separated. The impedance data were modeled with two parallel RC circuits in series using the nonlinear least-squares fitting program of the *Z-view* software to separate the grain and grain-boundary contributions from the electrode contribution to the impedance spectra.

An Arrhenius plot of the total (grain and grain-boundary) electrical conductivities of the samples is shown in Figure 13. The sample densities were 95 and 96% for formate and 92% for the carbonate. The data are in good agreement with the data for GDC10 previously reported by Steele<sup>15</sup> for a commercial clean GDC powder ( $SiO_2$ , 30 ppm) produced by Rhodia. Steele's data show slightly higher conductivity, but the activation energies ( $E_a$ ) are very similar. A small change in slope is observed around 400 °C that is associated with  $(Gd'_{Ce} - V''_O)$  complexes. Above 400 °C, the  $(Gd'_{Ce} - V''_O)$  complexes are dissociated, which gives rise to a

(14) (a) Scherrer, P. *Nachr. Ges. Wiss. Goettingen* **1918**, 2, 98. (b) Klug, H. P.; Alexander, L. E. *X-ray Diffraction Procedures for Polycrystalline and Amorphous Materials*, 2nd ed.; John Wiley & Sons: New York, 1974.

(15) Steele, B. C. H. *Solid State Ionics* **2000**, 129, 95.

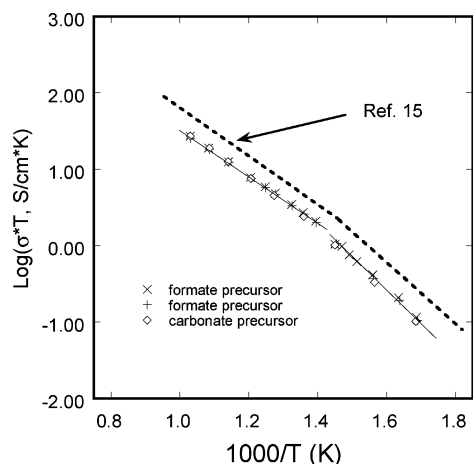


**Figure 13.** Comparison of electrical conductivity vs reciprocal temperature for GDC10 prepared from formate and carbonate precursors with data from the literature.<sup>15</sup>

activation energy of 0.61(1) eV lower than the value of 0.82(1) eV for the data below 400 °C (see Figure 13). The corresponding values from ref 15 are 0.64 and 0.79 eV.

### Conclusion

We have demonstrated a simple and inexpensive solid solution precursor route to GDC from a low-temperature solution with high yield and high purity using cerium nitrate and gadolinium nitrate as starting materials. This method provides an efficient way to produce high-quality material that can be densified at 1450 °C. The ionic conductivity of GDC obtained by the thermal decomposition of the precursors is comparable to the best result reported in the literature.

This systematic investigation on the influences of reactant and temperature on the yield and morphology of precursor

showed that the yield of precursor crystals increases with temperature and is slightly dependent on the reactants of  $\text{Ce}(\text{NO}_3)_3/\text{Gd}(\text{NO}_3)_3$ ,  $\text{Ce}(\text{NO}_3)_3/\text{Gd}(\text{OAc})_3$ ,  $\text{CeCl}_3/\text{Gd}(\text{NO}_3)_3$ , and  $\text{CeCl}_3/\text{Gd}(\text{OAc})_3$ . The particle size of the formate crystals prepared from the reflux method was decreased from 15  $\mu\text{m}$  (long needle) to 1–10  $\mu\text{m}$  (short hexagonal rod) when the reaction temperature was increased from 80 to 105 °C, whereas the sizes of crystals prepared from a static reaction were 50–200  $\mu\text{m}$  at 80 °C and 500  $\mu\text{m}$  at 105 °C. In contrast, carbonate precursors show different morphologies and sizes depending on the reactants, and the reaction temperature only affects the yield of precursor crystals. The particular gadolinium salt used in the synthesis plays a critical role in determining the morphology of carbonate precursor crystals.

The carbonate precursor route has advantages in terms of higher yield, the use of  $\text{H}_2\text{O}$  instead of DMF/ethanol as the solvent, lower decomposition temperature, and the smaller and more regular size of the precursor crystals. However, the carbonate precursor requires a higher calcination temperature than the formate precursor to prepare the GDC powder (850 °C vs 600 °C) to obtain dense ceramics at 1450 °C.

**Acknowledgment.** This research was partially supported by the State of Texas through the Texas Center for Superconductivity at the University of Houston, the R. A. Welch Foundation, and NSF Grant No. DMR-0502740. Gun Tae Kim is acknowledged for his help with the conductivity measurements.

**Supporting Information Available:** Crystallographic information in CIF and PDF format for compounds **1–3**. This material is available free of charge via the Internet at <http://pubs.acs.org>.

CM071310K